Nanometer-Scale Creation and Characterization of Trapped Charge in SiO_2 Films Using Ballistic Electron Emission Microscopy

B. Kaczer, Z. Meng, and J. P. Pelz
The Ohio State University, 174 W. 18th Ave., Columbus, Ohio 43210
(Received 8 November 1995)

Electron injection into ~25 nm thick SiO_2 films in $Pt/SiO_2/Si$ structures using ballistic electron emission microscopy (BEEM) is found to produce a local suppression in the BEEM current, which is at least partly due to electron trapping in the SiO_2 film. Measured variations in the BEEM threshold voltage with the voltage applied across the SiO_2 film can be used to estimate the local trapped electron density and the centroid location, which agree with macroscopic measurements. Our measurements indicate that BEEM can be sensitive to very small numbers of electrons trapped in buried SiO_2 films. [S0031-9007(96)00509-1]

PACS numbers: 61.16.Ch, 72.20.Jv, 73.40.Qv

Charge trapping phenomena in SiO_2 films are of great fundamental interest, as well as immense technological importance for the operation of metal-oxide-semiconductor field-effect transistor (MOSFET) devices [1–4]. While a variety of techniques have been developed to study different aspects of charge injection, electric field-induced carrier heating, trap creation, and carrier trapping [1,2], nearly all prior techniques give information which is spatially averaged over large sample areas. Only recently have Ludeke *et al.* [5–7] shown that the technique of ballistic electron emission microscopy (BEEM) [8] can be used to study electronic transport properties of thin (<10 nm) SiO_2 films in MOS structures with nanometer-scale spatial resolution. This opens up new possibilities for nanometer-scale studies of charge trapping in buried films of SiO_2 and other wide-band-gap materials.

We have used BEEM to locally inject and microscopically characterize trapped charge in MOS structures with moderately thick (~25 nm) oxide films. Electrons injected into the oxide conduction band produce a local *suppression* in the transmitted electron flux through the oxide film (BEEM current). This suppression increases with the total amount of injected charge, depends on the electric field across the oxide E_{ox} during injection, and is accompanied by an increase of the BEEM threshold voltage V_{th} indicating that it is related to charge trapping and/or damage *within* the oxide film, and not simply from hot electron damage at the metal-oxide interface [9]. By measuring variations of V_{th} with E_{ox}, we show that BEEM can be used to make *nanometer-scale* estimates of the trapped charge density and the charge centroid location, which are consistent with prior macroscopic measurements of charge trapping in SiO_2 films [1]. Our measurements suggest that BEEM is sufficiently sensitive to detect the trapping of a very small number of electrons ($\lesssim 10$) in buried oxide films.

All experiments were performed in an ultrahigh vacuum (UHV) system (base pressure $<2 \times 10^{-10}$ torr) equipped with a custom-built multipurpose scanning tunneling microscope (STM) [10] and an electron-beam evaporator. *p*-type Si(001) wafers (doping level of $\sim 1 \times 10^{15}$ cm^{-3}) with ~25 nm of high quality thermally-grown SiO_2 (provided by National Semiconductor Inc.) were cut into 5×20 mm^2 pieces, cleaned using a sequence of acetone, methanol, and deionized water rinses, and introduced into the UHV sample preparation chamber. MOS samples were made *in situ* using electron-beam evaporation [11] to deposit ~5 nm of Pt (measured with a quartz crystal microbalance) onto the oxide surface through a shadow mask, producing several "dots," each 1 mm in diameter. The sample was then passed in UHV to the STM, where a 0.1 mm thick Au wire was used to electrically ground a particular Pt dot. Electrochemically etched W tips were cleaned *in situ* with electron beam bombardment prior to the BEEM measurements.

The basic principle of the BEEM technique (discussed in Refs. [5] and [8]) is illustrated in Fig. 1. Under an applied tip bias V_T, "hot" electrons can be injected locally from the STM tip into a thin metal film. Most of these electrons will scatter, thermalize, and contribute only to the external current I_T. However, a fraction may propagate ballistically across the thin metal film [8], and some of these may be "injected" into the oxide conduction band provided they have sufficient energy to surmount the barrier at the metal-oxide interface [5–7]. These injected electrons may then be accelerated by an electric field in the oxide and/or be scattered by phonons [7,12], defects, or trapped charge. Some injected electrons will be scattered back into the metal film [5], some may become trapped in the oxide [1,2], and some may conduct across the oxide into the Si substrate and be measured as the "BEEM" or external collector current I_c. By monitoring I_c as a function of V_T, I_T, V_b, and past sample history, microscopic properties of oxide injection, carrier transport [5–7], and charge trapping may be studied.

The creation of a region of locally suppressed collector current I_c by BEEM electron injection is illustrated in Fig. 2. Figure 3 then demonstrates that this suppression is associated with trapped electrons in the oxide film. Figure 2(a) shows a $\sim 150 \times 150$ nm^2 STM topographic image of a "pristine" (i.e., with no prior scanning) area of

 © 1996 The American Physical Society

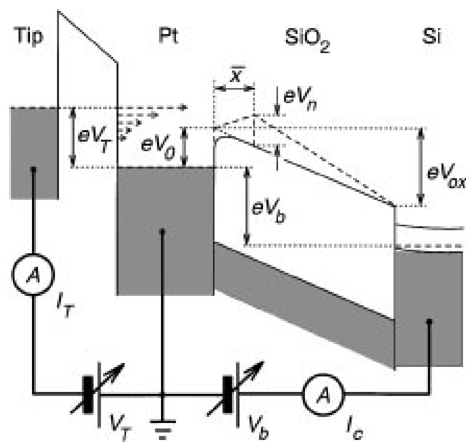

FIG. 1. Energy-level diagram of the experiment. The voltage V_T controls the energy of the hot electron flux (represented by dashed arrows) injected into the thin Pt film. Ballistic electrons which surmount the barrier near the metal-oxide interface and traverse the oxide film constitute the collector current I_c. The barrier can be modified by the applied bias V_b, and by trapped charge (assumed to be a uniform sheet, appearing as voltage V_n to the BEEM electrons) located at a distance $\overline{x}$ into the oxide film. The solid (dashed) line represents the oxide conduction band minimum without (with) trapped charge.

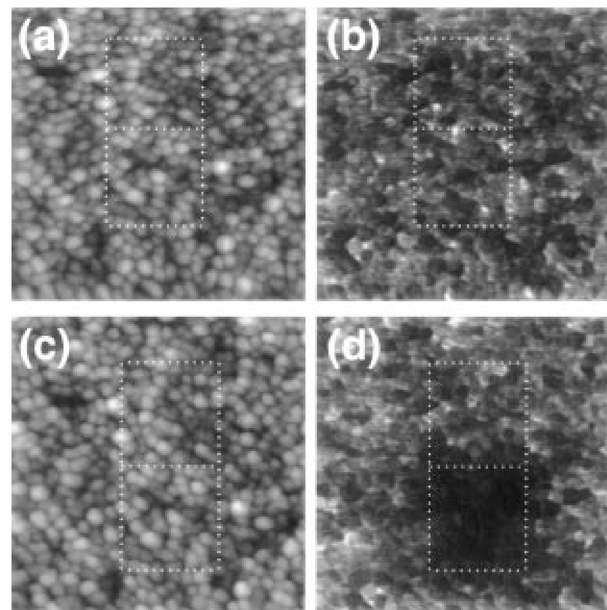

FIG. 2. Suppression of the collector current I_c caused by charge injection. (a) $\sim 150 \times 150$ nm^2 topographic scan before injection, measured with $V_T = 5.4$ V, $I_T \cong 10$ nA, and $V_b^{\mathrm{meas}} = 8$ V. The Pt topography (full gray-scale range 2.5 nm) shows a nodular character similar to that reported in Ref. [7]. (b) Corresponding BEEM image (gray-scale range 0–5 pA), (c) topography, and (d) BEEM image after injection (see text), over the two regions outlined by dashed lines. Injection in the upper region was done with a reverse oxide bias of $V_b^{\mathrm{inj}} = -4$ V. Injection in the lower region was done with a forward oxide bias of $V_b^{\mathrm{inj}} = +12$ V. Significant suppression is observed only for the forward-bias injected region.

the Pt metal surface, while Fig. 2(b) shows the simultaneously measured BEEM image (i.e., a plot of I_c vs tip position), measured with $V_T = 5.4$ V, $I_T \cong 10$ nA, and a "forward" oxide bias of $V_b^{\mathrm{meas}} = +8$ V (note voltage polarities are defined in Fig. 1). For these conditions $I_c > 0$, and the integrated collector charge density was measured to be $Q_c \cong 10-13$ C cm^{-2}. The BEEM image in Fig. 2(b) shows distinct contrast, which is in partial correlation with topographic features [7].

Next, two controlled "injection" scans were performed over two $\sim 50 \times 50$ nm^2 adjacent regions, whose locations on the sample are indicated by the dashed lines in Fig. 2. The actual injection scan was done by increasing V_T from 1 V to 5.4 V, then holding it for ~ 60 s at 25 equally spaced locations during each injection scan (with $I_T \cong 20$ nA), while I_c was recorded and integrated. The only difference between the lower and upper injected regions is that a forward oxide bias $V_b^{\mathrm{inj}} = +12$ V was applied over the lower region, while a reverse oxide bias $V_b^{\mathrm{inj}} = -4$ V was applied over the upper region. For forward oxide bias, the average integrated collector charge density was $Q_c \cong 125$ C cm^{-2}, while for reverse oxide bias it was negligible. We note that for the reverse oxide bias no I_c is expected since the BEEM electrons do not have sufficient energy to surmount both the ~ 4 eV barrier [5] at the metal oxide interface and the ~ 4 V reverse bias across the oxide film.

Finally, a $\sim 150 \times 150$ nm^2 "postinjection" scan was made using the same parameters as the "preinjection" scan. This is shown in Figs. 2(c) and 2(d). Several features are apparent from Fig. 2. (1) The long injection scan has caused no modification to the topography of the top metal surface, but has caused a significant local suppression of the current I_c through the oxide film. (2) The suppression is much stronger for the forward oxide bias injection than for the reverse oxide bias injection. By comparing the preinjection and postinjection BEEM images, we find that for forward bias $\langle I_c \rangle_{\mathrm{region}} \cong (25 \pm 5)\%$ of its value in the preinjection scan, while for reverse bias there is almost no detectable change, with $\langle I_c \rangle_{\mathrm{region}} \cong (95 \pm 5)\%$ of the original value.

We now consider two possible origins of the observed local suppression of I_c: (1) enhanced scattering of the BEEM electrons due to hot-electron induced interdiffusion at the metal-oxide interface (analogous to behavior observed by Hallen *et al.* [9] for certain Au/Si Schottky barrier samples), and (2) a local buildup of trapped electrons *within* the bulk of the oxide film. If in fact trapped electrons in the oxide are present near the suppressed region, then the electric field from this trapped charge should *increase* the energy barrier at the metal-oxide interface (see Fig. 1) [3], which in turn should produce an increase in the BEEM threshold voltage V_{th} [8]. On the other hand, if changes in electron scattering from interface interdiffusion were the only cause of the suppression, then one would expect *no* significant shift in barrier height, as was the case in the hot-electron-induced interface modification experiments reported by Hallen *et al.* [9] for the Au/Si system.

We have found that a large increase in V_{th} is in fact present in the suppressed regions in our MOS samples, giving strong evidence that trapped negative charge is

indeed present. First, the tip was moved to a pristine area, and an injection scan was performed (similar to that described above) with either a forward ($V_b^{\rm inj} = +12$ V) or reverse ($V_b^{\rm inj} = -4$ V) oxide bias during injection. Then a single BEEM I_c-V_T [8] curve was measured (with $I_T \cong 10$ nA and $V_b^{\rm meas} = +8$ V) at the center of the injected region. This procedure was repeated several times at different sample locations, and the corresponding I_c-V_T curves were averaged together. For comparison a number of well-spaced [13] I_c-V_T curves were also measured on entirely pristine sample areas. The top, middle, and bottom curves in Fig. 3 show these averaged I_c-V_T curves for pristine (p), reverse-bias (r), and forward-bias (f) injected regions, respectively, and the arrows indicate the corresponding fitted BEEM threshold voltages $V_{\rm th}$ for each curve (with typical uncertainty ± 0.1 V) [14]. With the oxide bias $V_b^{\rm meas} = +8$ V, we find $V_{\rm th}^p \cong 3.3$ V for the pristine areas. For the reverse-bias injected regions (which show at most mild suppression in Fig. 2) we find a slightly larger value $V_{\rm th}^r \cong 3.5$ V, while for the forward-biased injected regions (which show strong suppression) we find a significantly larger value of $V_{\rm th}^f \cong 4.6$ V. In general, we always find that injection-induced suppressed regions

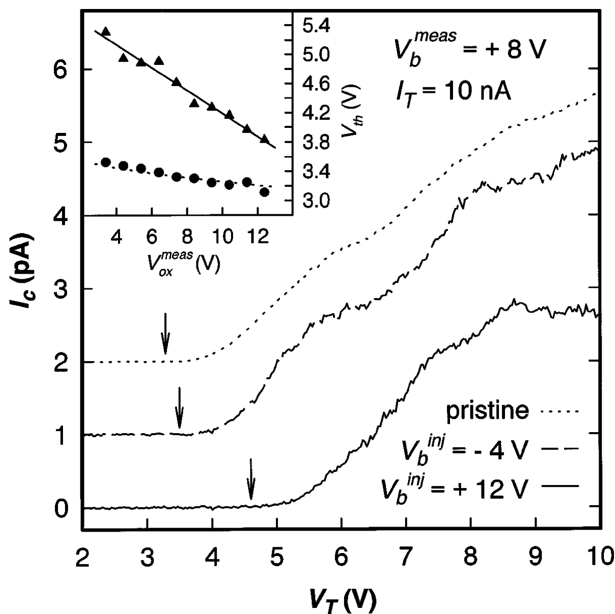

FIG. 3. Averaged I_c-V_T curves (100, 6, and 6 curves averaged, respectively) measured over pristine regions (dotted curve), reverse-bias injected regions (dashed curve), and forward-bias injected regions (full curve), respectively, with measured BEEM thresholds of $V_{\rm th} \cong 3.3$, 3.5, and 4.6 V, respectively. For clarity, the top two curves have been vertically offset. For the forward-bias injected regions a large increase in $V_{\rm th}$ and a suppression of I_c (at $V_T = 5.4$ V) are seen. Inset; Dependence of the threshold voltage $V_{\rm th}$ on $V_{\rm ox}^{\rm meas}$ applied during I_c-V_T curve measurements (note that $V_{\rm ox}^{\rm meas} \cong V_b^{\rm meas} - 0.6$ V in this voltage range [15]), for pristine (circles) and forward-bias injected (triangles) regions. Curves show model fits according to Eq. (1), with $V_0 \cong 3.8$ V, $\bar{x} \cong 3.9$ nm, and $n_{\rm trap} \cong 1.3 \times 10^{13}$ cm^{-2}.

are accompanied by a significant increase in $V_{\rm th}$, directly indicating that trapped negative charge is present.

We next show that we can use these BEEM threshold voltage shifts to make estimates of the *local* trapped-charge density in injected regions. In the simplest one-dimensional trapped-charge model, which assumes planar geometry and approximates the trapped electron density $n_{\rm trap}$ as a uniform sheet of negative charge located within the oxide film at a distance $\bar{x}$ from the metal-oxide interface (see Fig. 1), the expression for $V_{\rm th}$ (which corresponds to the maximum barrier height) is

$$V_{\rm th} = \begin{cases} V_0 - \bar{x}E_{\rm ox} + V_n & \text{if } V_n \geq \bar{x}E_{\rm ox}\,, \\ V_0 - \sqrt{(e/4\pi\varepsilon_d)(E_{\rm ox} - V_n/\bar{x})} & \text{if } V_n < \bar{x}E_{\rm ox}\,, \end{cases} \quad (1)$$

where $E_{\rm ox} = V_{\rm ox}/L$ is the applied electric field across the oxide without trapped charge, $V_{\rm ox} \cong V_b - 0.6$ V is the voltage drop across the oxide [15], $L \cong 25$ nm is the oxide film thickness, V_0 is the intrinsic barrier height at the metal-oxide interface (see Fig. 1), $V_n \equiv (en_{\rm trap}/\varepsilon_s)(L - \bar{x})\bar{x}/L$ (see Fig. 1) [16], $\varepsilon_s \cong 3.9\varepsilon_o$ and $\varepsilon_d \cong 2.15\varepsilon_o$ are the static and optical dielectric constants of the oxide film, respectively, $\varepsilon_0 = 8.85 \times 10^{-14}$ F cm^{-1}, and e is the elementary charge. For $V_n < \bar{x}E_{\rm ox}$, the electric field due to the trapped negative charge increases $V_{\rm th}$ by reducing the amount of "image force lowering" [4] of the barrier below $V_{\rm th}$ while for $V_n \geq \bar{x}E_{\rm ox}$ the total electric field near the metal-oxide interface is actually reversed and the barrier is increased above V_0.

According to this model, we should be able to directly determine the parameters V_0, $n_{\rm trap}$, and $\bar{x}$ by monitoring how $V_{\rm th}^p$ (measured over pristine areas) and $V_{\rm th}^f$ (measured after forward-bias injection) vary with the oxide bias $V_b^{\rm meas}$ applied during measurement of the I_c-V_T curve. The inset of Fig. 3 shows fits from Eq. (1) with the parameter values $V_0 \cong 3.8$ V, $\bar{x} \cong 3.9$ nm, and $n_{\rm trap} \cong 1.3 \times 10^{13}$ cm^{-2} (note that $n_{\rm trap} = 0$ is assumed for pristine areas). We see that both $V_{\rm th}^p$ and $V_{\rm th}^f$ are fit very well by this simple model. $V_{\rm th}^p$ exhibits the effect of image force lowering [4,17] and the value $V_0 \cong 3.8$ V is close to that ($\cong$3.9 V) reported by Ludeke *et al.* [5–7] for the Pt/SiO_2 interface. The extracted parameter values for $\bar{x}$ and $n_{\rm trap}$ for the forward-bias injected region are in quite reasonable agreement with past macroscopic measurements [1] of charge buildup in SiO_2 films under similar injection conditions (i.e., with $E_{\rm ox} = 11.4$ V/25 nm $\cong 4.6$ MV cm^{-1}, and injected charge density of $Q_c \cong 125$ C cm^{-2}).

While the measurements shown in Fig. 3 provide strong evidence that trapped charge is present in the suppressed regions, they do not prove that the trapped charge is the *only* cause of the suppression. It is possible that part of the suppression is due to enhanced scattering resulting from damage (either in the top metal layer, at the metal-oxide interface, or within the oxide bulk) which occurs simultaneously with a buildup of trapped charge in the oxide. We note here that the observation that suppression is much stronger under forward-bias than reverse-bias injections (as shown in Fig. 2) gives supporting evidence that processes

within the oxide bulk are more likely to be the major cause of suppression than any interdiffusion at the metal-oxide interface or creation of point defects in the top metal layer [9]. This is because any change in the electric field created by V_b is mostly confined to the oxide region and is shielded from the metal film. Therefore the local potential "seen" by hot BEEM electrons in the metal layer and at the metal-oxide interface (and hence their kinetic energy and net number) should be essentially *independent of* V_b, and one would expect similar damage rates under both forward and reverse biases. The fact that suppression can be "turned off" under reverse oxide bias then suggests that scattering due to either creation of defects in the metal layer or enhanced interface interdiffusion is not a significant cause of the suppression. We add that this conclusion follows only if we make the "local" assumption that any hot-electron induced damage in the metal layer or at the metal-oxide interface depends only on the local electron kinetic energy and is independent of the shape of the potential deep in the oxide. Such an assumption seems reasonable since the strong inelastic electron-phonon scattering in the SiO_2 bulk [7,12] will largely wash out quantum-mechanical phase interference effects which may couple the electronic wave function in the metal and at the metal-oxide interface to the potential in the oxide bulk. We note that Ludeke *et al.* [5–7] have made a similar assumption concerning electron transport (namely, that transport processes across the interface are essentially independent from processes in the oxide bulk).

On the other hand, the fact that the suppression is much stronger under forward-bias injection agrees well with the proposed trapping and/or damage mechanisms *within* the oxide bulk. Forward bias will increase the number of BEEM electrons entering the oxide (through image force lowering of the barrier [4]), and will increase their average kinetic energy (via field-induced electron "heating" [1,2]), which in turn should increase trap creation and/or other hot-electron-induced damage with the oxide film.

Based on our estimates of the trapped charge density in suppressed regions, we can also estimate the total number of trapped electrons in a given region. We see that the strongly suppressed region in Fig. 2 contains only about $(50\ \mathrm{nm})^2 \times (1.3 \times 10^{13}\ \mathrm{cm}^{-2}) \cong 325$ trapped electrons, which corresponds to fewer than 15 trapped electrons for each of the 25 I_c-V_T/I_c-t curves used for injection. Similarly, from other "BEEM image" scans following charge injection (with $V_T = 10$ V) at a *single* location (not shown), we find our samples that the measured suppression in I_c is localized to a region $\sim$15–25 nm across. Assuming the trapped electron density of $\sim 1.3 \times 10^{13}\ \mathrm{cm}^{-2}$ spread over such an area, we conclude that only about $\sim$25–65 trapped electrons can produce *significant* local suppression of I_c, corresponding to a typical decrease in I_c of up to $\sim$10 pA. We therefore conclude that BEEM is sensitive to a very small number of trapped electrons in the oxide below the tip. Ultimately, we believe that it should be possible to use BEEM to observe even *individual* electron trapping or detrapping events.

In summary, we show that charge trapping in SiO_2 films accompanies injection of BEEM electrons into the oxide and that is at least partially responsible for local suppression of the BEEM current. We have also shown that BEEM can be used to make nanometer-scale measurements of the local trapped charge density and the approximate depth of the trapped charge in the oxide.

The authors wish to thank Darrell Jones for technical assistance and advice, and Carlos Egues and Robert Perry for useful discussions. This work is supported by Office of Naval Research Grant No. N00014-93-0607, and by NSF Grant No. DMR93-57535.

[1] D. J. DiMaria, and J. W. Stastiak, J. Appl. Phys. **65**, 2342 (1989).

[2] D. J. DiMaria, E. Cartier, and D. Arnold, J. Appl. Phys. **73**, 3367 (1993).

[3] E. H. Nicollian and J. R. Brews, *MOS Physics and Technology* (John Wiley and Sons, New York, 1982).

[4] S. M. Sze, *Physics of Semiconductor Devices* (John Wiley and Sons, New York, 1981).

[5] R. Ludeke, A. Bauer, and E. Cartier, Appl. Phys. Lett. **66**, 730 (1995).

[6] R. Ludeke and A. Bauer, J. Vac. Sci. Technol. A **13**, 614 (1995).

[7] R. Ludeke, A. Bauer, and E. Cartier, J. Vac. Sci. Technol. B **13**, 1830 (1995).

[8] W. J. Kaiser and L. D. Bell, Phys. Rev. Lett. **60**, 1406 (1988); L. D. Bell and W. J. Kaiser, Phys. Rev. Lett. **61**, 2368 (1988).

[9] H. D. Hallen *et al.,* J. Vac. Sci. Technol. B **9**, 585 (1991); A. Fernandez *et al.,* Appl. Phys. Lett. **57**, 2826 (1990).

[10] D. E. Jones, J. P. Pelz, Y. H. Xie, P. J. Silverman, and G. H. Gilmer, Phys. Rev. Lett. **75**, 1570 (1995).

[11] R. Ludeke has reported (private communication) that radiation damage during *e*-beam deposition caused severe breakdown in his very thin ($\sim$5 nm) oxide films. We have found no problem with oxide breakdown with our thicker (25 nm) oxide films for *e*-beam depositions done at an acceleration voltage of 4.1 kV.

[12] M. V. Fischetti and D. J. DiMaria, in *The Physics and Technology of Amorphous* SiO_2, edited by R. A. B. Devine (Plenum, New York, 1988), p. 160.

[13] Measurement of an I_c-V_T curve leaves behind a small amount of trapped charge, which can then be sensed if a subsequent I_c-V_T curve is taken nearby. It is therefore important to keep I_c-V_T curves well separated ($\gtrsim$25 nm) to minimize this effect [B. Kaczer and J. P. Pelz (to be published)].

[14] V_{th} was determined by fitting the above-threshold region of the I_c-V_T curves with an assumed $I_c \propto (V_T\text{-}V_{\mathrm{th}})^{2.5}$ dependence (see Ref. [5]).

[15] This assumes a Pt-Si work-function difference of 0.45 V and corrects for band banding effects in the *p*-type Si substrate (see Refs. [4] and [7]).

[16] D. J. DiMaria, J. Appl. Phys. **47**, 4073 (1976).

[17] A. Davies and H. G. Craighead, Appl. Phys. Lett. **64**, 2833 (1994).